JOURNAL OF OPTOELECTRONICS AND ADVANCED MATERIALS Vol. 12, No. 1, January 2010, p. 52 - 56

Beam self-trapping by pyroelectric effect

M. CHAUVET*, J. SAFIOUI, F. DEVAUX
Département d'Optique, Institut FEMTO-ST, UMR CNRS 6174, Université de Franche-Comté, 25030 Besançon, France

Optical beam self-trapping induced by pyroelectric effect is demonstrated in a photorefractive medium. A 10 degree temperature raise of a lithium niobate crystal is shown to be sufficient to self-trap a 15µm diameter beam at 532nm. The phenomenon is explained by the local screening of the internal pyroelectric field produced by the spontaneous polarisation change. Such an optical nonlinearity can lead to the formation of 2-D spatial pyroelectric solitons. Experimental demonstrations are confirmed by numerical calculations.

(Received December 15, 2009; accepted January 20, 2010)

Keywords: Photorefractive effect, Self-trapping, Spatial soliton, Pyroelectric effect

1. Introduction

Beam self-trapping has attracted a lot of interest since the introduction of the concept [1] and the first experimental observation of stable trapping by Kerr effect [2]. The search for versatile and efficient nonlinear focusing medium is still of interest. Quadratic medium [3], liquid crystals [4] or photorefractive (PR) medium [5] are able to give rise to self-confined beams that keep a constant transverse profile upon propagation. Such beams are called spatial solitons [6-11]. Spatial solitons with specificities such as two frequency components or different host material such as solitons formed in nematic liquid crystals have been discovered. Among those, photorefractive spatial solitons have attracted much attention [8-11] because of their appealing features. For instance, they can be created at very low light power level and are stable in 2-D due to the saturating character of the nonlinearity. Nevertheless, application of a strong external applied electric field is, most often, a necessary condition to obtain the local PR nonlinearity required in light trapping experiments [12]. This drawback is not present in the case of photovoltaic photorefractive crystals [13,14] but control of the photorefractive nonlinearity sign and amplitude is challenging [15] since the photovoltaic field is intrinsic to the crystal and is primarily intensity independent. In this paper we instead propose to use the spontaneous polarisation of ferroelectric crystal to induce a nonlinear optical effect which can be controlled using the pyroelectric effect. The concept of pyroelectric photorefractive beam self-trapped beams that can be formed by simple adjustment of the PR crystal temperature is introduced. Experimental demonstrations performed in lithium niobate ($LiNbO_3$) samples are presented.

2. Model

Pyroelectric crystals exhibit a variation in spontaneous polarisation P_s as a function of temperature change given by its pyroelectric coefficient $p=\partial Ps/\partial T$. In short-circuit crystal this spontaneous polarisation change is known to induce transient electric currents fruitfully utilized in wide bandwidth pyroelectric photodetectors. In open-circuit configuration very high electric field can be generated by pyroelectric effect. Such large electric field induced in the surrounding of pyroelectric crystal can be used to ionise and accelerate charged particles [16-17]. Recently, steady-state temperature gradient was shown to suppress photorefractive damage in $LiNbO_3$ [18]. In this letter internal electric field generated by a temperature change ΔT in an open-circuit crystal is considered. This electric field variation E_{py} due to the spontaneous polarisation change is given by:

$$E_{py} = \Delta E = -\frac{1}{\varepsilon_0 \varepsilon_r} p \Delta T. \qquad (1)$$

where ε_0 and ε_r are the vacuum and relative dielectric constants, respectively. Note that in a ferroelectric crystal at equilibrium the net internal field inside the crystal is null since the field due to spontaneous polarisation is compensated by charges accumulated on crystal faces. However temperature change induces direct spontaneous polarisation variation and thus electric field E_{py}. This field is not immediately compensated and a drift current can consequently take place as if an external voltage was applied to the crystal. The idea behind the concept of pyroelectric spatial soliton is to locally screen this initial homogeneous pyroelectric electric field E_{py} using the PR effect in order to induce beam self-trapping. Several conditions have to be fulfilled to allow beam self-focusing. For instance, once a crystal temperature is set, the induced pyroelectric field has to remain long enough compare to PR response time. Charge sorption on the polar surface of the crystal that progressively tends to compensate the temperature induced E_{py} has thus to be slower than the response time of the light-induced beam self-trapping. Moreover, the amplitude of E_{py} has to be large enough to induce efficient trapping for a moderate temperature change compatible with PR effect.

To model beam self-trapping in pyroelectric photorefractive crystal we consider a time-dependent band-transport model [19] with a single deep trap. Electrons which are dominant free charges are displaced by photovoltaic effect and under drift current along the crystal c-axis while diffusion is neglected. An open-circuit

crystal at homogeneous and steady temperature is considered.

When illuminated with a light intensity distribution I, evolution of the charge density ρ is given by:

$$\frac{\partial \rho}{\partial t} = -\mu e \vec{\nabla}\left(N.\vec{E}\right) - \beta_{ph}\vec{\nabla}[(N_d - N_d^+)I]\cdot\vec{c}. \quad (2)$$

where free electron density N, ionized donor density N_d^+ and internal electric field $\vec{E}$ are given by equations (3), (4) and (5), respectively

$$N = \frac{s(I+I_d)(N_d - N_d^+)}{\gamma N_d^+}. \quad (3)$$

$$N_d^+ = N_a + \frac{\rho}{e}. \quad (4)$$

$$\vec{E}(\vec{r}) = E_{py}.\vec{c} + \frac{1}{4\pi\,\varepsilon_0\varepsilon_r}\iiint_V \rho(\vec{r}')\frac{\vec{r}-\vec{r}'}{\left|\vec{r}-\vec{r}'\right|^3}dV. \quad (5)$$

N_d is the total donor density; N_a is the density of ionized shallow acceptors. $I_d=\beta/s$ is the equivalent dark irradiance with β and s the thermal and photoexcitation coefficients, γ is the recombination coefficient, μ is the electron mobility, β_{ph} is the photovoltaic coefficient and e is electron charge. Note that temperature change of the crystal due to illumination is neglected.

The electric field evolution is obtained by solving iteratively the set of equation (2-5) [20] in conjunction with the wave propagation equation. Starting from initial conditions, the electron density is calculated from eq. (3) and space charge variation after a time step Δt is deduced from eq. (2). Then the ionized donor density is obtained from eqs. (4). The electric field is deduced from eq. (5). The inferred 2-D refractive index perturbation Δn due to linear electro-optic effect is finally used to calculate light propagation along y-axis in the perturbed medium by a classical split-step Fourier transform method according to the nonlinear propagation equation.

$$\left\{\frac{\partial}{\partial y} - \frac{i}{2k}\Delta_\perp\right\}A = i\,k\Delta n\,A. \quad (6)$$

where $\Delta_\perp = \partial^2/\partial x^2 + \partial^2/\partial z^2$ is the transverse operator, A is the slowly-varying amplitude of the light field and k is the wavenumber in the medium.

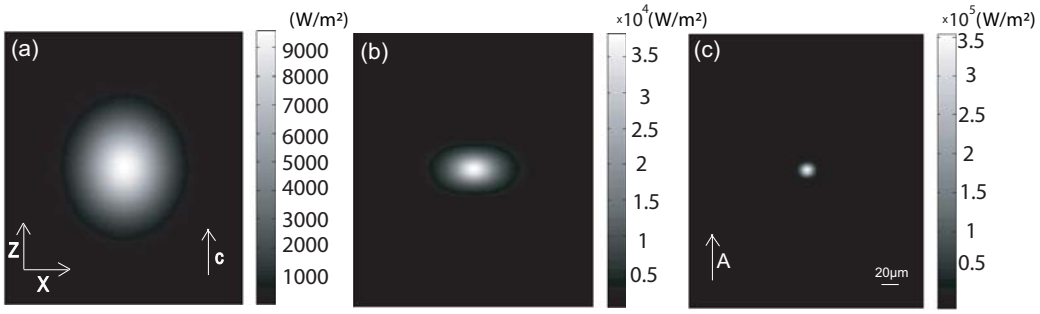

Fig. 1. Numerical simulation of beam self-trapping dynamics of an extraordinary polarised beam in a 20 mm long $LiNbO_3$ crystal. Output face in linear regime (a), output face in nonlinear regime at $t=t_F$ for best focusing (c) and at $t=t_F/2$ (b). Parameters: 80µw beam power, input beam power 16µm FWHM, ΔT=20°C, E_{ph}=36kV/cm.

To illustrate the concept of pyroelectric beam self-trapping we selected the widely available ferroelectric $LiNbO_3$ crystal. It possesses well-known PR properties along with a pyroelectric coefficient p close to -6.10^{-5} C m^{-2} K^{-1} at 25°C [21, 22]. The pyroelectric field E_{py} is oriented along the crystal c-axis (z-axis) and can be either positive or negative by increase or decrease of the crystal temperature, respectively. From Eq. (1) an amplitude of 47 kV/cm can be deduced for the internal pyroelectric electric field E_{py} under a temperature increase of 20°C. A linearly polarized beam propagating along the crystal y-axis can sense the light-induced refractive index distribution $\Delta n = -0.5n^3 r_{eff} E_z$. Where E_z is the electric field component along the crystal c-axis, n is average refractive index and r_{eff} is the effective electro-optic coefficient. Two configurations are analyzed, n_o=2.3 and r_{13}=8pm/V for ordinary polarized light and n_e=2.2 and r_{33}=31pm/V for extraordinary polarized light. Undoped $LiNbO_3$ crystals are used for the experimental demonstration and a single iron deep center is considered in the model. Corresponding parameters are taken from ref. [23].

Fig. 1 depicts the predicted behavior of an extraordinary polarized beam, with a 16µm (FWHM) width at the entrance face, propagating in a 20 mm long $LiNbO_3$ crystal whose temperature has been raised 20°C above initial temperature. When light is switched on progressive self-focusing is observed (Fig. 1b) until best confinement is reached (Fig. 1c).

Self-trapping is due to the photorefractive screening of the pyroelectric field in the central part of the beam. As a consequence where light is more intense the field amplitude approaches the photovoltaic field E_{ph} [24]. A waveguide structure is created in the crystal providing E_{py} is larger than E_{ph}. In the presented simulation E_{ph} is set to 36kV/cm and an extraordinary polarized light is considered. The beam is finally narrower at the exit face

than at the input face. The anisotropic index distribution gives a slightly elliptical beam with a stronger confinement along c-axis. Self-trapping is also possible with ordinary polarization despite the weaker electro-optic value r_{13} thanks to a lower value of the photovoltaic field E_{ph} that allows to form a deeper space charge field [24].

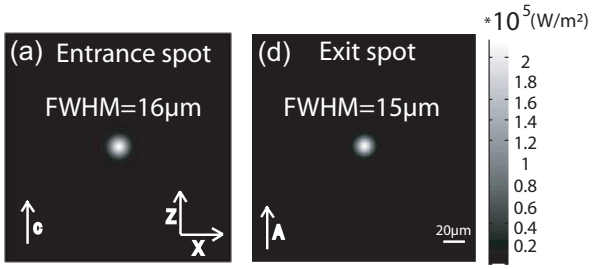

Fig. 2 Numerical simulation showing the formation of an extraordinary polarized pyroelectric soliton in a 20mm long $LiNbO_3$ sample. Input (a) and output beam intensity distribution for best focusing time (b). Parameters: 80µW input beam power, 16 µm beam FWHM, ΔT = 10 °C, E_{ph}=19kV/cm.

Note that for adequate parameters a circular beam with a similar width than the launched beam can be obtained at the exit face of the crystal when best confinement is reached which corresponds to a solitonic propagation. The case of an extraordinary 16µm FWHM soliton beam is presented in Fig. 2.

3. Experiments

For the experimental demonstration either undoped photonic grade congruent or stoichiometric $LiNbO_3$ crystals are used. Samples cut from photonic grade z-cut wafers have dimensions 8×20×0.5 mm^3 along x, y and z crystallographic axes, respectively. The sample under test is placed between an insulating plastic cover and a metallic plate whose temperature is accurately controlled by a Peltier element. Such an arrangement provides a homogeneous temperature of the crystal with stability better than 0.1°C. Input and output faces of the crystal are observed on a CCD camera via imaging lenses.

A first experiment is performed with extraordinary polarized light in a stoichiometric $LiNbO_3$ crystal (Fig. 3). A 532nm CW beam is focused to a 11µm FWHM spot at the front face (Fig. 3a) and propagates over 20mm along the $LiNbO_3$ y-axis direction. When the crystal is at room temperature the beam diffracts along propagation, its width at the output face is close to 500 µm which corresponds the crystal thickness (Fig. 3b) as witnessed by the Lloyd interferences produced by reflection on the c-faces of the crystal. Moreover its spatial distribution is not Gaussian since no spatial filter was used to clean the launched beam. Nevertheless when the crystal temperature is raised from room temperature to 40°C the 80µW beam self-focuses progressively. As shown in Fig. 3d beam confinement and clean-up are already obvious after 1 min of exposure while crystal temperature is not yet stabilized. As predicted by the numerical model, trapping is more efficient along the z-axis than along x-axis which is clearly observed in Fig. 2e. When maximum confinement ($t=t_F$) is reached a smooth and efficiently focused spot is obtained (Fig. 3f) with a 7 µm FWHM along c-axis and a 8 µm FWHM along x-axis. The large initial beam diffraction has thus been overcompensated which illustrates the remarkable self-trapping efficiency triggered by the spontaneous polarisation of the crystal.

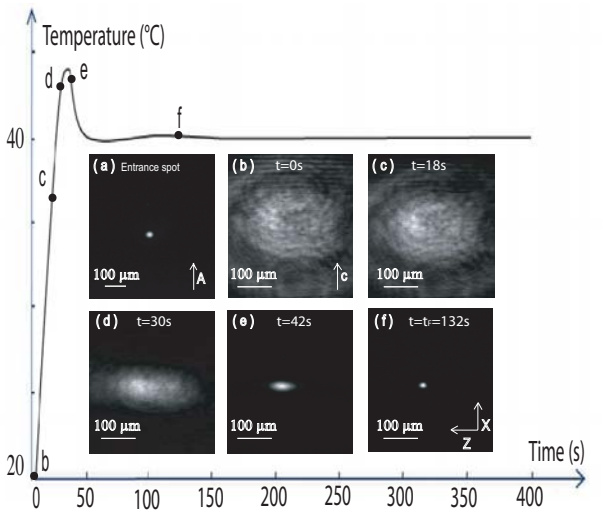

Fig. 3. Pyroelectric self-focusing dynamics of an extraordinary polarized beam at λ=532 nm in a 20mm long stoichiometric $LiNbO_3$ crystal for ΔT=20°c. Crystal temperature evolution (curve) and images at the input face (a) and at the output face at different instant indicated on the curve (b-f). Parameters: 80µW input beam power, 11 µm input beam FWHM.

To show the influence of light polarisation, experiments have also been performed for ordinary light as exposed in Fig. 4. Optimum confinement leads to tighter beam for extraordinary polarisation than for ordinary polarisation as expected from theory. Uncertainties on the value of crystal parameters prohibit quantitative prediction of the time evolution but the overall behaviour is correctly described by our numerical calculation. Note that the induction time to reach best focusing ($t=t_F$) is dependent on light polarization. We measured t_F=2 min (Fig. 3f) or t_F=7 min (Fig. 4f) for extraordinary or ordinary polarisation, respectively. This response time disparity can be attributed to the photorefractive field which has larger amplitude for ordinary light and thus takes a longer time to build-up [24]. In addition the photoionization cross section can be polarisation dependent because of crystal anisotropy [25].

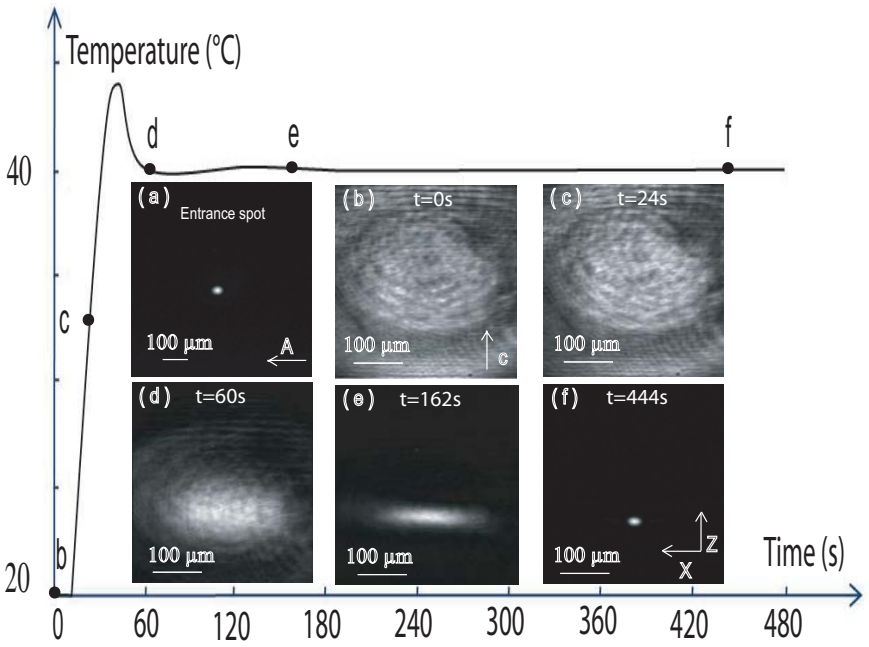

Fig. 4. Pyroelectric self-focusing dynamics of an ordinary polarized beam at λ=532 nm in a 20mm long stoichiometric $LiNbO_3$ crystal for ΔT=20°c. Crystal temperature evolution (curve) and images at the input face (a) and at the output face at different instant indicated on the curve (b-f). Parameters are identical as in Fig.3.

Note that self-trapping can also be obtained when crystal temperature is stabilized for several minutes before beam is switched on. Since this last procedure is more consistent with the assumptions of our theoretical model it is used as a standard procedure in the following experiment. Assessment of the focusing strength at different time after temperature is set leads to an internal pyroelectric field decay rate τ of about 12h in our lithium niobate crystals. This slow decay due to the compensation of E_{py} is consistent with the dielectric response time of $LiNbO_3$ in the dark.

Additional experiments obtained in congruent $LiNbO_3$ samples show similar behaviour than in stoichiometric samples. To illustrate this and, simultaneously, to demonstrate a solitonic propagation, experimental results are presented in Fig. 5. Indeed, for a given temperature change ΔT, which is the experimental parameter that dictates the amplitude of the nonlinear effect, the beam profile to launch in order to obtain propagation with an invariant transverse profile can be determined as shown in Fig. 2. An extraordinary polarized 15µm FWHM pyroelectric soliton is demonstrated when crystal temperature is raised 10°C above room temperature as witnessed by the similar beam profile at the input (Fig. 5a) and output (Fig. 5b) faces of the crystal. Note that these solitons are obtained in quasi-steady-state regime [9] since longer exposure time shows beam broadening. A solution to form steady-state narrow solitons could be to artificially increase the dark irradiance with the help of a uniform background illumination as for screening solitons [8]. Also note that once spatial soliton is formed, beam can be switched off and crystal can be reset to room temperature without altering the induced guiding structure. Due to the high resistivity of $LiNbO_3$ long living waveguides are thus memorised in the crystal and can thus be practically used to guide low power beams at different wavelengths. Indeed photorefractive effect is negligible for low power visible beam or at near I.R. telecommunication wavelengths. In such a situation induced waveguides are memorized even if $LiNbO_3$ sample temperature changes.

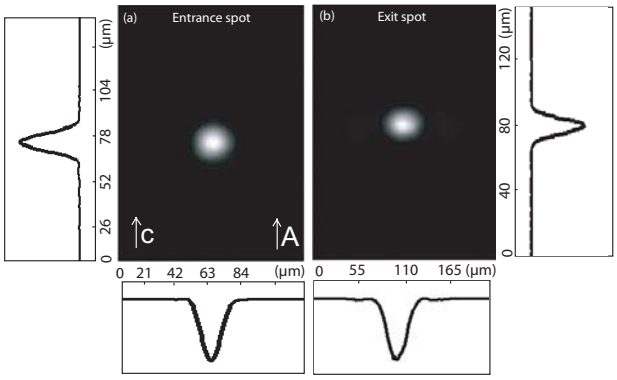

Fig. 5 Experimental demonstration of an ordinary polarised pyroelectric soliton in a congruent $LiNbO_3$ sample. Input (a) and output (b) beam intensity distribution for best focusing time. Parameters: 80 µW input beam power, 15 µm beam FWHM, ΔT = 10 °C.

4. Conclusion

The concept of beam self-trapping using spontaneous polarisation of ferroelectric crystal has been presented. Amplitude and sign of the nonlinear focusing effect is simply controlled by crystal temperature via the pyrolectric effect. Experimental demonstrations have been performed in $LiNbO_3$ crystals and pyroelectric spatial solitons have been obtained. Photonic grade undoped congruent or stoichiometric $LiNbO_3$ samples reveal efficient beam self-confinement under moderate temperature change on the order of 10°C. This powerful and easy to control optical nonlinearity can be advantageously employed to induce structures such as gratings, complex lattices or 3-D integrated circuits even inside large size medium. It is important to note that the reported effect could potentially be obtained in other pyroelectric photorefractive crystals providing characteristics such as long pyroelectric field decay time and large enough pyroelectric field amplitude are present.

References

[1] R. Y. Chiao, E. Garmire, C. H. Townes, Phys. Rev. Lett **13**, 479 (1964).
[2] A. Barthélémy, S. Maneuf, C. Froehly, Opt. Comm **55**, 201 (1985).
[3] K. Hayata, M. Koshiba, Phys. Rev. Lett **71**, 3275 (1993).
[4] M. Peccianti, A. De Rossi, G. Assanto, A. De Luca, C. Umeton, I. C. Khoo, Appl. Phys. Lett **77**, 7 (2000).
[5] G. Duree, J. L. Shultz, G. J. Salamo, M. Segev, A. Yariv, B. Crosignani, P. Di Porto, E. J. Sharp, R. R. Neurgaonkar, Phys Rev. Lett **71**, 533 (1993).
[6] A. D. Boardman and A. P. Sukhorukov, Soliton Driven Photonics (Kluwer Acad. Publ., Dordrecht, 2001).
[7] S. Trillo, W. E. Torruellas, Spatial Solitons (Springer-Verlag, Berlin, 2001).
[8] M. Segev, G. C. Valley, B. Crosignani, P. Di Porto, A. Yariv, Phys. Rev. Lett **73**, 3211 (1994).
[9] M. Morin, G. C. Duree, G. J. Salamo, M. Segev, Opt. Lett **20**, 2066 (1995).
[10] D. Neshev, E. Ostrovkaya, Y. Kivshar, W. Krolokowski, Opt. Lett **28**, 710 (2003).
[11] W. Krolikowski, M. Saffman, B. Luther-Davies, C. Denz, Phys. Rev. Lett **80**, 3240 (1998).
[12] E. Fazio, F. Renzi, R. Rinaldi, M. Bertolotti, M. Chauvet, W. Ramadan, A. Petris, V. I. Vlad, Appl. Phys. Lett **85**, 2193–2195 (2004).
[13] M. Taya, M. C. Bashaw, M. M. Fejer, M. Segev, G. C. Valley, Phys. Rev. A **52**, 3095 (1995).
[14] W. L. She, K. K. Lee, W. K. Lee, Phys. Rev. Lett **83**, 3182 (1999).
[15] C. Anastassiou, M. F. Shih, M. Mitchell, Z. Chen, M. Segev, Opt. Lett **23**, 924 (1998).
[16] J. D. Brownridge, Nature **358**, 277 (1992).
[17] J. Geuther, Y. Danon, F. Saglime, Phys. Rev. Lett **96**, 054803 (2006).
[18] S. M. Kostritskii, O. G. Sevostyanov, M. Aillerie, P. Bourson, J. Appl. Phys **104**, 114104 (2008).
[19] P. Günter, J. P. Huignard, Photorefractive materials and their applications 2 (Springer, Berlin, 2007).
[20] F. Devaux, V. Coda, M. Chauvet, R. Passier, J. Opt. Soc. Am. B **25**, 1081 (2008).
[21] T. Bartholomaüs, K. Buse, C. Deuper, E. Krätzig, Phys. Stat. Sol.(a) **142**, K55 (1994).
[22] A. Savage, J. Appl. Phys **37**, 3071 (1966).
[23] M. Simon, S. Wevering, K. Buse, E. Krätzig, J. Phys. D **30**, 144 (1997).
[24] J. Safioui, M. Chauvet, F. Devaux, V. Coda, F. Pettazzi, M. Alonzo, E. Fazio, J. Opt. Soc. Am. B. **26**, 487- 492 (2009).
[25] G. Montemezzani, C. Medrano, P. Günter, Phys. Rev. Lett **79**, 3403-3406 (1997).

*Corresponding author: mathieu.chauvet@univ-fcomte.fr